Molecular Plant
Research Article

CellPress
PARTNER JOURNAL

GIGANTEA Shapes the Photoperiodic Rhythms of Thermomorphogenic Growth in *Arabidopsis*

Young-Joon Park[1,4], Jae Young Kim[1,4], June-Hee Lee[1], Byoung-Doo Lee[2], Nam-Chon Paek[2,3] and Chung-Mo Park[1,3,*]

[1]Department of Chemistry, Seoul National University, Seoul 08826, Korea

[2]Department of Plant Science, Seoul National University, Seoul 08826, Korea

[3]Plant Genomics and Breeding Institute, Seoul National University, Seoul 08826, Korea

[4]These authors contributed equally to this article.

***Correspondence: Chung-Mo Park (cmpark@snu.ac.kr)**

https://doi.org/10.1016/j.molp.2020.01.003

ABSTRACT

Plants maintain their internal temperature under environments with fluctuating temperatures by adjusting their morphology and architecture, an adaptive process termed thermomorphogenesis. Notably, the rhythmic patterns of plant thermomorphogenesis are governed by day-length information. However, it remains elusive how thermomorphogenic rhythms are regulated by photoperiod. Here, we show that warm temperatures enhance the accumulation of the chaperone GIGANTEA (GI), which thermostabilizes the DELLA protein, REPRESSOR OF *ga1-3* (RGA), under long days, thereby attenuating PHYTOCHROME INTERACTING FACTOR 4 (PIF4)-mediated thermomorphogenesis. In contrast, under short days, when GI accumulation is reduced, RGA is readily degraded through the gibberellic acid-mediated ubiquitination-proteasome pathway, promoting thermomorphogenic growth. These data indicate that the GI–RGA–PIF4 signaling module enables plant thermomorphogenic responses to occur in a day-length-dependent manner. We propose that the GI-mediated integration of photoperiodic and temperature information shapes thermomorphogenic rhythms, which enable plants to adapt to diel fluctuations in day length and temperature during seasonal transitions.

Key words: thermomorphogenesis, day length, GI, RGA, PIF4

Park Y.-J., Kim J.Y., Lee J.-H., Lee B.-D., Paek N.-C., and Park C.-M. (2020). GIGANTEA Shapes the Photoperiodic Rhythms of Thermomorphogenic Growth in *Arabidopsis*. Mol. Plant. **13**, 459–470.

INTRODUCTION

It is widely accepted that global warming, a gradual increase in average global temperatures, places significant pressure on ecosystems and vegetation (Huang et al., 2017). Under global warming, the synchronization of day-length information and temperature cues is frequently disturbed during seasonal transitions, causing abnormal growth and development in a variety of crop species (Peng et al., 2004). Therefore, it is essential to understand how these external stimuli are integrated into intrinsic regulatory networks, by which plants timely and adequately adapt to fluctuating environments.

Plants undergo a distinct array of morphological and architectural changes in response to warm temperatures, such as hypocotyl elongation, increased leaf hyponasty, formation of thin leaves, and accelerated flowering, which are collectively termed thermomorphogenesis (Koini et al., 2009; Franklin et al., 2011; Park et al., 2019). These morphogenic traits are known to facilitate dissipation of body heat and evaporative leaf cooling (Crawford et al., 2017; Park et al., 2019), facilitating plant adaptation to warm temperatures. In recent years, the genes and associated molecular mechanisms governing thermomorphogenic responses in various plant species have been discovered (Franklin et al., 2011; Delker et al., 2014; Box et al., 2015; Park et al., 2017).

It is known that warm temperatures lead to hypocotyl thermomorphogenesis via the E3 ubiquitin ligase CONSTITUTIVE PHOTOMORPHOGENIC 1 (COP1) (Delker et al., 2014; Park et al., 2017). Notably, thermo-induced hypocotyl elongation occurs during a specific period of time in the day (Box et al., 2015; Jung et al., 2016; Park et al., 2017). Of particular interest is the fact that thermomorphogenic rhythms are coordinated by day-length information, peaking around midday under long days (LDs; 16-h light and 8-h dark) but at the end of the night

Published by the Molecular Plant Shanghai Editorial Office in association with Cell Press, an imprint of Elsevier Inc., on behalf of CSPB and IPPE, CAS.

under short days (SDs; 8-h light and 16-h dark) (Box et al., 2015; Park et al., 2017). These observations suggest that plants possess specific day-length-monitoring mechanisms that are capable of shaping the diel rhythms of thermomorphogenic responses.

The sensory mechanisms and physiological roles of day-length information in photoperiodic flowering have been studied extensively, whereby the timing of flowering induction depends on the length of the daytime (Song et al., 2012). The plant-specific GIGANTEA (GI) protein plays a crucial role in the induction of photoperiodic flowering (Sawa et al., 2007). GI interacts with the F-box protein FLAVIN-BINDING, KELCH REPEAT, F-BOX 1 (FKF1) in a blue-light-dependent manner, thereby reducing the protein stability of CYCLING DOF FACTOR 1 (CDF1), which acts as a floral repressor (Sawa et al., 2007). Interestingly, recent reports have shown that GI also functions as a chaperone in the maturation of the E3 ubiquitin ligase ZEITLUPE (ZTL), which acts as a circadian photoreceptor under blue-light conditions (Kim et al., 2011; Cha et al., 2017). It is therefore logical to expect that GI conveys photoperiodic information to regulators of distinct physiological processes by shielding substrate proteins from the ubiquitin-mediated degradation process.

Gibberellic acid (GA) is an agronomically important plant growth hormone that regulates diverse aspects of plant growth and development, such as seed germination, cell elongation, and flowering induction (Davière and Achard, 2013). A group of DELLA domain-containing proteins, including REPRESSOR OF *ga1-3* (RGA), GIBBERELLIC ACID INSENSITIVE (GAI), RGA-LIKE 1 (RGL1), RGL2, and RGL3, acts as transcriptional regulators that suppress GA responses and signaling (Tyler et al., 2004). Meanwhile, GA binds to its receptor protein GA INSENSITIVE DWARF1 (GID1), facilitating the interactions of the GID1 and DELLA proteins (Griffiths et al., 2006). The GID1–GA–DELLA complex subsequently interacts with the SCF E3 ubiquitin ligase complex to trigger the ubiquitin-mediated degradation of DELLA proteins (Dill et al., 2004).

It is remarkable that the DELLA proteins suppress the function of the growth-promoting transcription factors PHYTOCHROME INTERACTING FACTORs (PIFs) by sequestering their DNA-binding motifs or by reducing their protein abundances through the ubiquitin-proteasome pathway (de Lucas et al., 2008; Feng et al., 2008; Li et al., 2016). The literature reports that at warm temperatures, PIF4 directly activates the expression of the *YUCCA8* (*YUC8*) gene, which encodes an auxin biosynthetic enzyme, thus promoting hypocotyl elongation (Franklin et al., 2011). DELLA-mediated GA signaling exhibits circadian rhythms under SDs (Arana et al., 2011). Furthermore, GI interacts with the *Arabidopsis O*-fucosyltransferase SPINDLY (SPY) (Tseng et al., 2004), which activates DELLA by promoting SPY–PIF interactions (Zentella et al., 2017). Considering the notion that the rhythms of plant thermomorphogenic growth are shaped by day-length information, the question remains as to how photoperiod-sensing mechanisms are functionally linked to the DELLA-mediated regulation of PIF4 during thermomorphogenesis.

In this work, we demonstrated that the molecular chaperone GI shapes the photoperiodic rhythms of thermomorphogenic growth by thermostabilizing the GA-signaling mediator RGA, which acts as a suppressor of PIF4 function. Although GI abundance is relatively higher under LDs, it is lower under SDs. The GI-assisted thermostabilization of RGA is therefore prominent under LDs, resulting in attenuated thermomorphogenic growth. In contrast, the stabilization of RGA is diminished under SDs, further promoting thermomorphogenic growth. The GI-mediated photoperiodic shaping of thermomorphogenic rhythms provides an adaptation strategy by which plants retain thermomorphogenic growth at an appropriate level under LDs but promote it to a higher level under SDs. This thermomorphogenic process contributes to the efficient capture of sunlight under day-length conditions with relatively less daily light, in addition to the enhancement of leaf cooling (Nozue et al., 2007; Park et al., 2017).

RESULTS

GIGANTEA-Deficient *gi-2* Mutants Exhibit Overgrowth at Warm Temperatures

Recent thermomorphogenic studies have proposed an external coincidence model, in which temperature and photoperiodic cues are intricately integrated to trigger hypocotyl thermomorphogenesis during a specific time of the day (Park and Park, 2017; Martínez et al., 2018). In accordance with this model, phytochrome photoreceptors have been proved to function as thermosensors (Jung et al., 2016). In addition, the photomorphogenic promoter PIF4 plays a central role in thermomorphogenic responses (Koini et al., 2009). However, it still remains unsolved how day-length information modulates the diel patterning of thermomorphogenic growth.

While screening for genes that mediate photoperiodic sensing, it was observed that *Arabidopsis* GI-deficient *gi-2* mutants exhibited altered thermomorphogenic phenotypes, such as hypocotyl overgrowth, a wider leaf span, and an elevated leaf angle, in comparison with wild-type Columbia-0 (Col-0) plants (Figure 1A–1D). Complementation of *gi-2* mutants by expressing the *GI* gene driven by its own promoter restored hypocotyl growth to a level comparable with that observed in Col-0 plants at 28°C (Figure 1E). These observations indicate that a lack of functional GI is responsible for thermo-induced overgrowth in *gi-2* mutants.

The hypersensitive thermomorphogenic traits observed in the *gi-2* mutants were not evident in mutant plants that are defective in CONSTANS (CO), FLOWERING LOCUS T (FT), ZEITLUPE (ZTL), or SALT OVERLY SENSITIVE 2 (SOS2) (Figure 1F), which function downstream of GI, indicating that the thermomorphogenic roles of GI are functionally distinct from the previously identified roles of GI in flowering time control, circadian rhythmicity, and salt-tolerance modulation (Kim et al., 2007, 2013; Sawa and Kay, 2011; Song et al., 2012).

Thermal acceleration of hypocotyl elongation is primarily driven by the increased action of auxin (Sun et al., 2012). It was found that exogenous application of 1-*N*-naphthylphthalamic acid (NPA), a potent auxin transport inhibitor, suppressed the hypersensitive thermomorphogenic hypocotyl growth of *gi-2* mutants (Figure 2A). In addition, gene expression analysis

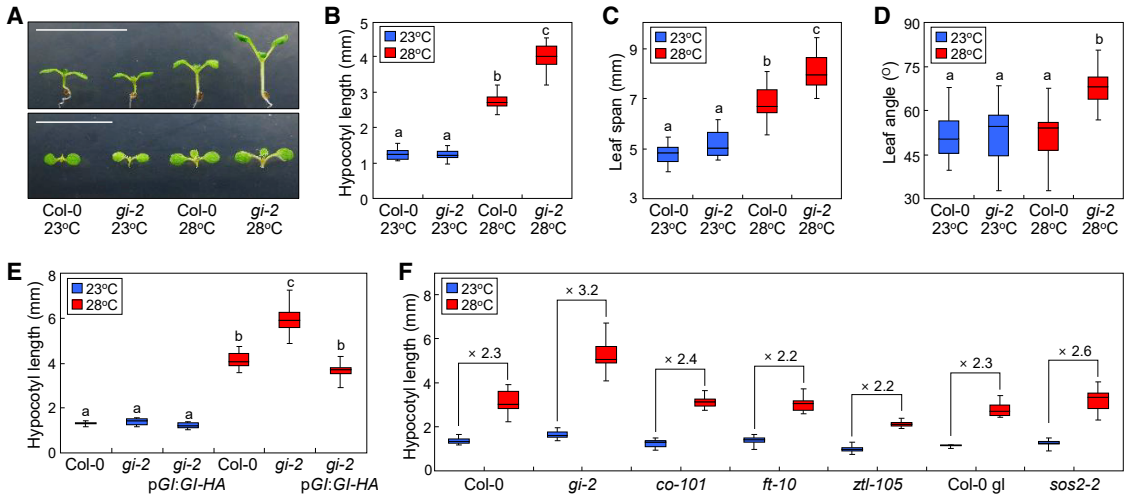

Figure 1. GIGANTEA-Deficient *gi-2* Mutants Exhibit Overgrowth at Warm Temperatures.

Different letters represent significant differences ($P < 0.05$) determined by one-way analysis of variance (ANOVA) with post hoc Tukey test. Three-day-old seedlings grown at 23°C under long days (LDs, 16-h light and 8-h dark) were subjected to temperature treatments for 4 days.

(A) Thermomorphogenic phenotypes. Side and top views of seedlings are displayed (upper and lower panels, respectively). Scale bar, 1 cm.

(B) Hypocotyl elongation.

(C) Leaf growth.

(D) Leaf hyponastic movement. Leaf angles relative to the horizontal plane were measured.

(E) Complementation of *gi-2* mutants. The p*GI:GI-HA* construct was transformed into *gi-2* mutants.

(F) Thermomorphogenic responses of *Arabidopsis* mutants harboring mutations in GI target genes. Numbers indicate fold changes. The *sos2-2* mutants are in the Col-0 gl background.

revealed that genes encoding the auxin biosynthetic enzyme YUCCA8 (YUC8) and the auxin-responsive protein SMALL AUXIN UPREGULATED RNA 22 (SAUR22) were greatly upregulated in *gi-2* mutants at warm temperatures (Figure 2B and 2C). In particular, the thermal induction of *YUC8* expression was more prominent in *gi-2* seedlings than in Col-0 seedlings, mostly during zeitgeber time (ZT) 16–24, ZT 40–48, and ZT 64–72 (Figure 2B; Supplemental Figure 1A and 1B). Furthermore, *gi-2* seedlings still grew during ZT 16–24 at 28°C (Figure 2D and 2E), which is the same period as thermomorphogenic growth occurs in wild-type seedlings under SDs (see below) (Box et al., 2015; Park et al., 2017). Together, these observations indicate that auxin responses are elevated in *gi-2* mutants at warm temperatures.

GI-Mediated Thermomorphogenic Responses Require PIF4

The PIF4 transcription factor acts as the master regulator of auxin-directed thermomorphogenic growth (Koini et al., 2009; Sun et al., 2012). It was therefore examined whether GI is functionally linked to PIF4 in terms of triggering thermomorphogenic responses. Notably, the *pif4-101* mutation was epistatic to the *gi-2* mutation (Figure 2F). In addition, molecular genetic studies showed that the greater thermal induction of the *YUC8* and *SAUR22* genes in *gi-2* mutants was mostly compromised in *gi-2 pif4-101* double mutants, similar to what was observed in *pif4-101* mutants (Figure 2G). These observations indicate that GI requires PIF4 in mediating thermomorphogenic hypocotyl growth.

Meanwhile, gene expression assays revealed that the transcription of *PIF4* and its closest homolog *PIF5* was altered to some degree in *gi-2* seedlings (Supplemental Figure 1C and 1D). However, it is unlikely that this degree of transcriptional distinction is sufficient to explain the dramatic effects of GI on the transcription of PIF4 target genes (Figure 2B and 2C), as has been noted previously (Nohales et al., 2019). In addition, the differential expression patterns of *PIF4* and *PIF5* were not strongly correlated with the diel expression patterns of the *YUC8* and *SAUR22* genes in *gi-2* mutants (Figure 2B and 2C; Supplemental Figure 1C and 1D). These gene expression data suggest that the effects of the GI–PIF4 association during thermomorphogenesis are exerted at the post-translational level.

GI is a critical constituent of the photoperiodic flowering genetic pathway (Sawa et al., 2007; Yu et al., 2008). It also plays a role in low-temperature-responsive flowering (Jang et al., 2015). PIF4 is also known to promote flowering (Kumar et al., 2012). Therefore, potential interactions between GI and PIF4 in flowering time control were explored. It was found that the flowering time of *gi-2* mutants was largely insensitive to warm temperatures, and the flowering time of *gi-2 pif4-101* double mutants was comparable with that of *gi-2* mutants (Supplemental Figure 1E), indicating that GI-mediated thermomorphogenic responses are functionally distinct from the role of GI in the timing of induction of flowering.

GI Is Associated with the Thermostabilization of RGA

Interestingly, hypocotyl thermomorphogenesis assays on several *gi* mutant alleles, namely *gi-1*, *gi-2*, and *gi-201* (Figure 3A), all of which exhibit severely late flowering (Martin-Tryon et al., 2007; Yu et al., 2008), revealed that these alleles result in differential thermomorphogenic responses. While the thermomorphogenic hypocotyl growth of *gi-1* mutants was comparable with that of wild-type Col-0 seedlings, *gi-201* and *gi-2* mutants exhibited

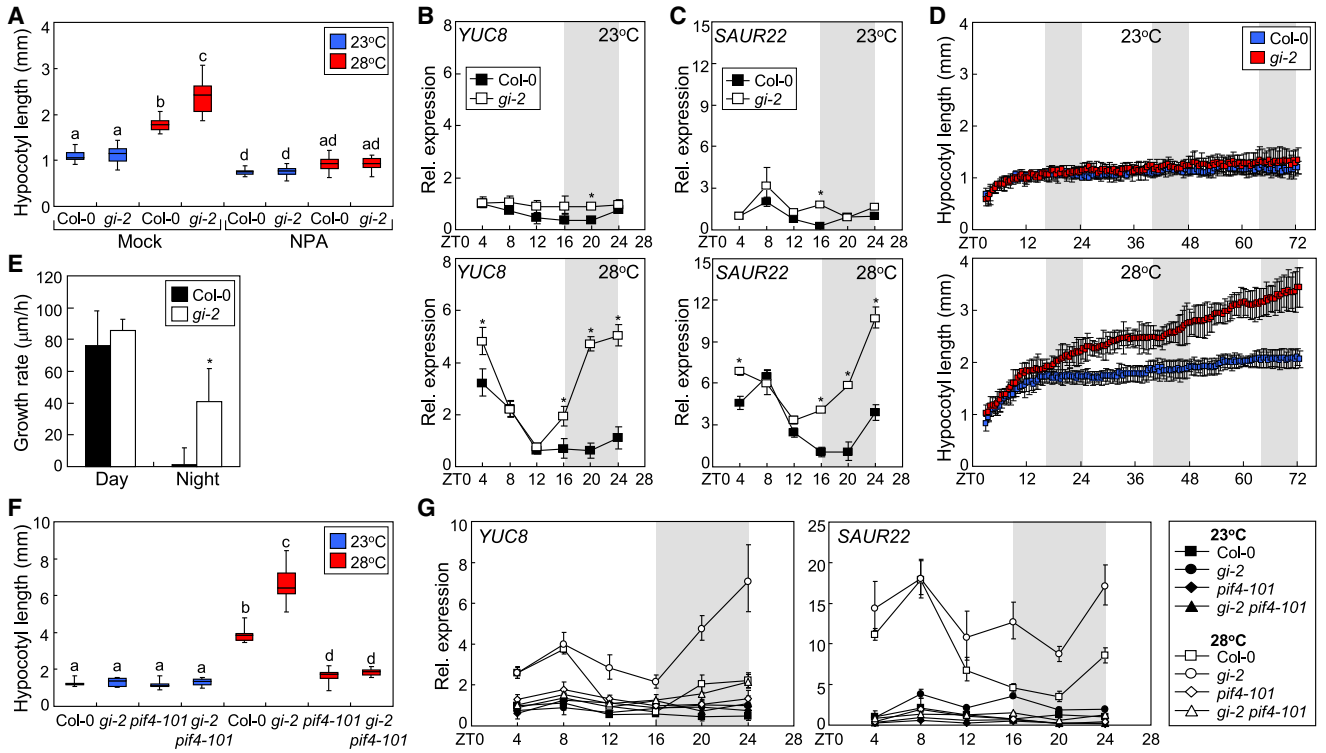

Figure 2. GI-Mediated Thermomorphogenic Responses Require PIF4.

(A) Effects of NPA on thermomorphogenic hypocotyl growth. Three-day-old seedlings grown at 23°C under LDs were subjected to temperature treatments for 4 days. Different letters represent significant differences ($P < 0.05$) determined by one-way ANOVA with post hoc Tukey test. NPA was included at a final concentration of 10 mM in growth medium.

(B and C) Diel patterns of *YUC8* **(B)** and *SAUR22* **(C)** transcription. Five-day-old seedlings grown under LDs were temperature-treated for 1 day. Whole seedlings were harvested at the indicated zeitgeber time (ZT) points for total RNA extraction. Transcript levels were analyzed by qRT–PCR. Biological triplicates, each consisting of 15 independent seedlings, were statistically analyzed (*t*-test, $^*P < 0.01$, difference from Col-0). Error bars indicate standard error of the mean (SE). See also Supplemental Figure 1.

(D and E) Kinetics of hypocotyl elongation. **(D)** Two-day-old seedlings grown under LDs were subjected to temperature treatments for up to 3 days. **(E)** Average growth rates during the first daytime (ZT 4–12) and nighttime (ZT 16–24) periods were calculated. Biological triplicates, each consisting of 15 independent seedlings, were analyzed (*t*-test, $^*P < 0.01$, difference from Col-0). Error bars indicate SE.

(F) Thermomorphogenic hypocotyl growth in *gi-2 pif4-101* mutants. Hypocotyl lengths of seedlings grown under LDs were statistically analyzed, as described in Figure 1B. See also Supplemental Figure 1.

(G) Diel expression patterns of *YUC8* and *SAUR22* genes. Seedlings were grown and qRT–PCR was performed as described above. Error bars indicate SE. See also Supplemental Figure 1.

hypersensitive hypocotyl growth in response to warm temperatures (Figure 3B). These observations are consistent with the notion that GI-mediated thermomorphogenic responses are functionally distinct from GI-mediated flowering time control. The *gi-1* mutant harbors a mutation in the C-terminal region of GI, while the *gi-2* and *gi-201* mutants contain mutations in the N-terminal region of GI (Figure 3A). It is therefore likely that the N-terminal region of GI is essential for thermomorphogenic responses, whereas both the N-terminal and C-terminal regions of GI are involved in flowering time control. It has been proposed that the N-terminal region of GI possesses a general chaperone activity that facilitates the maturation of ZTL proteins (Kim et al., 2007; Cha et al., 2017). It is expected that the N-terminal domain of GI, and perhaps also its intrinsic chaperone activity, are critical for the thermomorphogenic regulation of hypocotyl growth.

The DELLA proteins, which are key regulators of GA signaling, are potential substrates of GI chaperone activity. It is known that DELLA protein abundance is diurnally regulated by the 26S proteasome pathway in a GA-dependent manner (de Lucas et al., 2008; Feng et al., 2008). Notably, it has been shown that DELLA regulators suppress the activity of PIF transcription factors by reducing their DNA-binding capability and through promoting their degradation via the ubiquitin-proteasome pathway (de Lucas et al., 2008; Li et al., 2016). In conjunction with the elevated transcription of PIF4 targets in *gi-2* mutants, such as *YUC8* and *SAUR22*, it was hypothesized that GI is involved in stabilizing the DELLA proteins at warm temperatures.

It was found that the levels of RGA protein, a representative DELLA protein, were significantly lowered in *gi-2* mutants (Figure 3C and Supplemental Figure 2). In addition, the RGA protein levels were not discernibly lower in the warm-temperature-treated *gi-2* mutants when a potent GA biosynthesis inhibitor, paclobutrazol (PAC), was included in the growth medium (Figure 3D and Supplemental Figure 2), suggesting that GI attenuates the GA-induced degradation of

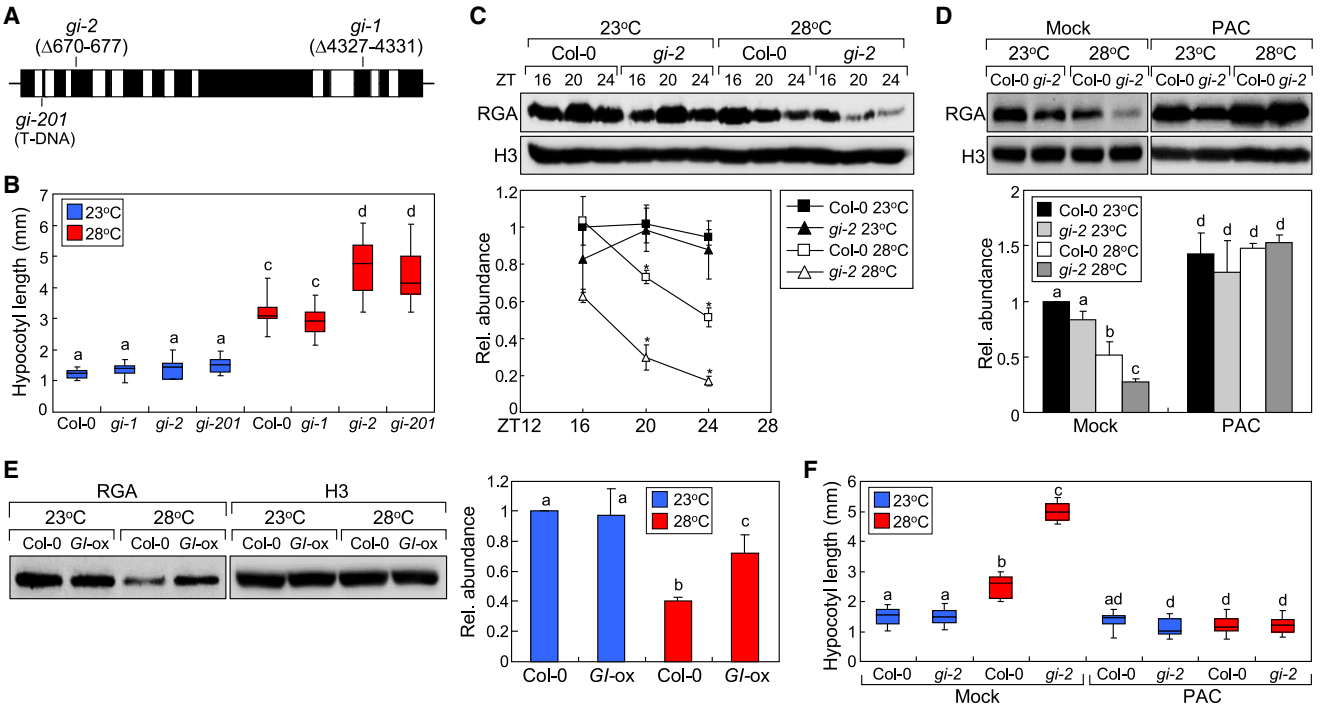

Figure 3. GI Is Associated with the Thermostabilization of RGA.

(A) Genetic mapping of *gi* alleles. Black boxes denote exons and white boxes denote introns.

(B) Effects of *gi* alleles on thermomorphogenic hypocotyl growth. Three-day-old seedlings grown at 23°C under LDs were subjected to temperature treatments for 4 days. Different letters represent significant differences ($P < 0.05$) determined by one-way ANOVA with post hoc Tukey test.

(C) Protein abundance of RGA in *gi-2* mutants. Seedlings were grown under LDs, as described in Figure 2B, and whole seedlings were harvested at ZT 16, 20, and 24 for total protein extraction. RGA and H3 proteins were immunodetected using anti-RGA and anti-H3 antibodies, respectively. Biological triplicates, each consisting of 15 independent seedlings, were statistically analyzed using Student's *t*-test (*$P < 0.01$, difference from Col-0 23°C). Error bars indicate SE. See also Supplemental Figures 2 and 3.

(D) Effects of PAC on RGA protein accumulation. Seedlings grown in the presence of 0.2 mM PAC under LDs were harvested at ZT 24. Total protein extraction and immunodetection of RGA and H3 were performed, as described above. Different letters represent significant differences ($P < 0.05$) determined by one-way ANOVA with post hoc Tukey test.

(E) Protein abundance of RGA in *GI*-overexpressing (*GI*-ox) seedlings. Seedling growth, total protein extraction, and immunodetection of RGA and H3 were performed, as described above.

(F) Effects of PAC on thermomorphogenic hypocotyl growth. Seedlings grown under LDs were treated with 0.2 mM PAC, as described above. See also Supplemental Figure 4.

RGA protein. We also found that the RGA proteins were relatively more stable in 35S:*GI* transgenic seedlings than in Col-0 seedlings at 28°C (Figure 3E), further supporting that GI thermostabilizes the RGA protein. Meanwhile, gene expression assays revealed that the transcript levels of *DELLA* genes were not discernibly affected in *gi-2* mutants (Supplemental Figure 3). Together, these observations indicate that GI mediates the thermostabilization of RGA.

It has been shown that DELLA proteins promote the degradation of PIF transcription factors (Li et al., 2016). Therefore, the diel rhythms of PIF4 protein abundance in *gi-2* mutants were examined. Notably, PIF4 protein levels were higher in *gi-2* mutants compared with Col-0 seedlings during the nighttime when grown at 28°C (Supplemental Figure 2), which is consistent with the thermomorphogenic hypocotyl phenotype of *gi-2* mutants. In addition, the PIF4 protein levels were reduced in the presence of PAC, as has been reported previously (Li et al., 2016). These findings indicate that the GI-mediated stabilization of RGA proteins is linked with PIF4 protein abundance during hypocotyl thermomorphogenesis.

We next asked whether the thermostabilization of RGA proteins is functionally associated with thermomorphogenic responses. It has previously been shown that hypocotyl thermomorphogenesis is compromised in *gid1a gid1c* mutants that lack GA receptors (Stavang et al., 2009). We found that the thermomorphogenic hypocotyl growth of *rga-28* and *rga-28 gai-t6* mutants was comparable with that of Col-0 seedlings (Supplemental Figure 4A). In contrast, the hypocotyls of *dellaq* mutants, which are defective in the *RGA*, *GAI*, *RGL1*, and *RGL2* genes, were much longer than those of L*er* seedlings at both 23°C and 28°C (Supplemental Figure 4B), suggesting functional redundancy among DELLA members. In addition, transcription of the *YUC8* and *SAUR22* genes was higher in the *dellaq* mutants compared with L*er* plants (Supplemental Figure 4C), indicating that RGA, as well as other DELLA members, play a critical role in hypocotyl thermomorphogenesis. While the hypocotyl lengths of *gi-2* and Col-0 seedlings were similar at 23°C, the hypocotyls of the *dellaq* seedlings were longer than those of L*er* seedlings even at 23°C. This phenotypic distinction is because GI stabilizes DELLA proteins mainly at 28°C. Notably, the hypersensitive thermomorphogenic growth of *gi-2* hypocotyls disappeared in the

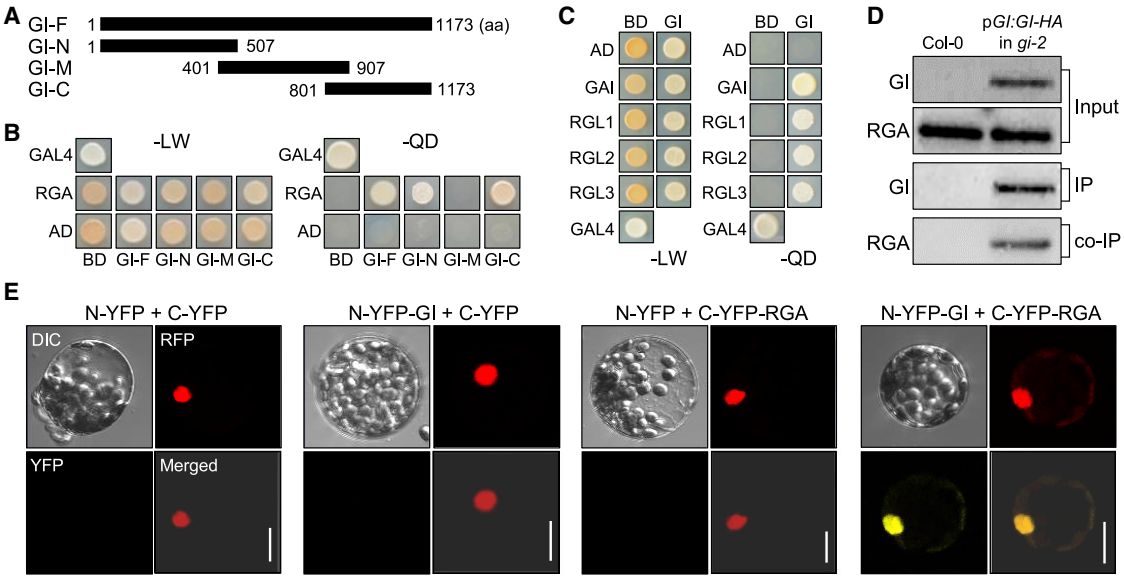

Figure 4. GI Interacts with RGA.

(A) GI constructs. Numbers indicate amino acid (aa) positions.

(B and C) Interactions of GI with DELLA proteins. -LW indicates Leu and Trp dropout plates. -QD indicates Leu, Trp, His, and Ade dropout plates. Interactions of GI with RGA **(B)** and other DELLA members **(C)** were examined in yeast cells. 3-Amino-1,2,4-triazole (3-AT; 20 mM) was included in growth medium.

(D) CoIP analysis of GI–RGA interaction. Six-day-old p*GI:GI-HA gi-2* seedlings grown at 23°C under LDs were harvested at ZT 24. GI and RGA proteins were immunodetected using anti-HA and anti-RGA antibodies, respectively.

(E) BiFC analysis of GI–RGA interaction in the nucleus. Yellow fluorescence indicates positive GI–RGA interaction. Red fluorescent protein–SPEECHLESS (RFP-SPCH) fusion was used as nuclear marker. Cell morphology was visualized by differential interference contrast (DIC) microscopy. Scale bars, 20 mm.

presence of PAC (Figure 3F), where RGA protein is stable (Figure 3D). Furthermore, the thermal induction of the *SAUR22* gene in *gi-2* mutants was diminished when seedlings were treated with PAC (Supplemental Figure 4D). Taken together, these observations indicate that the GI-mediated thermostabilization of RGA is intimately associated with thermomorphogenic responses.

GI Interacts with DELLA

Upon discovering the role of GI in RGA thermostabilization, we examined whether GI directly interacts with RGA using a group of GI constructs with different protein domains (Figure 4A). Yeast two-hybrid assays showed that the N-terminal and C-terminal regions of GI (residues 1–507 and 801–1173, respectively), but not the central region (residues 401–907), interact with RGA (Figure 4A and 4B). The efficient interaction between the N-terminal region of GI, which possesses a molecular chaperone activity (Cha et al., 2017), and RGA is related to the unaltered thermomorphogenic responses of *gi-1* mutants, in which part of the C-terminal region of GI is deleted (Figure 3A).

GI also interacted with other DELLA members, namely GAI, RGL1, RGL2, and RGL3 (Figure 4C), suggesting that GI is broadly functionally linked with GA–DELLA–PIF4 signaling events during thermomorphogenic responses.

The GI–RGA interactions *in planta* were further confirmed by co-immunoprecipitation (coIP) assays (Figure 4D). In addition, bimolecular fluorescence complementation (BiFC) assays revealed that GI and RGA interact with each other in the nucleus (Figure 4E). Collectively, these observations illustrate that GI modulates GA signaling during hypocotyl thermomorphogenesis by thermostabilizing RGA and other DELLA members through direct protein–protein interactions.

GI Incorporates Day-Length Information into Thermomorphogenesis

The functional roles of GI in the induction of photoperiodic flowering have been extensively studied (Sawa et al., 2007; Yu et al., 2008). As the rhythms of thermomorphogenic growth are modulated by photoperiod, we explored whether GI converts day-length information into thermomorphogenic hypocotyl growth.

Gene expression analysis revealed that the transcript levels of the *GI* gene were moderately elevated at 28°C under LDs, while the effects of warm temperature were somewhat irregular under SDs (Supplemental Figure 5A). Meanwhile, the overall levels of GI proteins were significantly lower under SDs, and, consistent with the previous finding that GI is degraded by the E3 ubiquitin ligase COP1 in the dark (Yu et al., 2008), the levels of GI proteins were rapidly reduced in darkness (Figure 5A and 5B), suggesting that the functional roles of GI are more prominent under LDs. In addition, RGA proteins were highly unstable at 28°C and the GI-assisted stabilization of RGA was compromised under SDs (Supplemental Figure 5B and 5C). Together, these observations indicate that GI converts photoperiodic information into the thermal stabilization of RGA proteins. It is

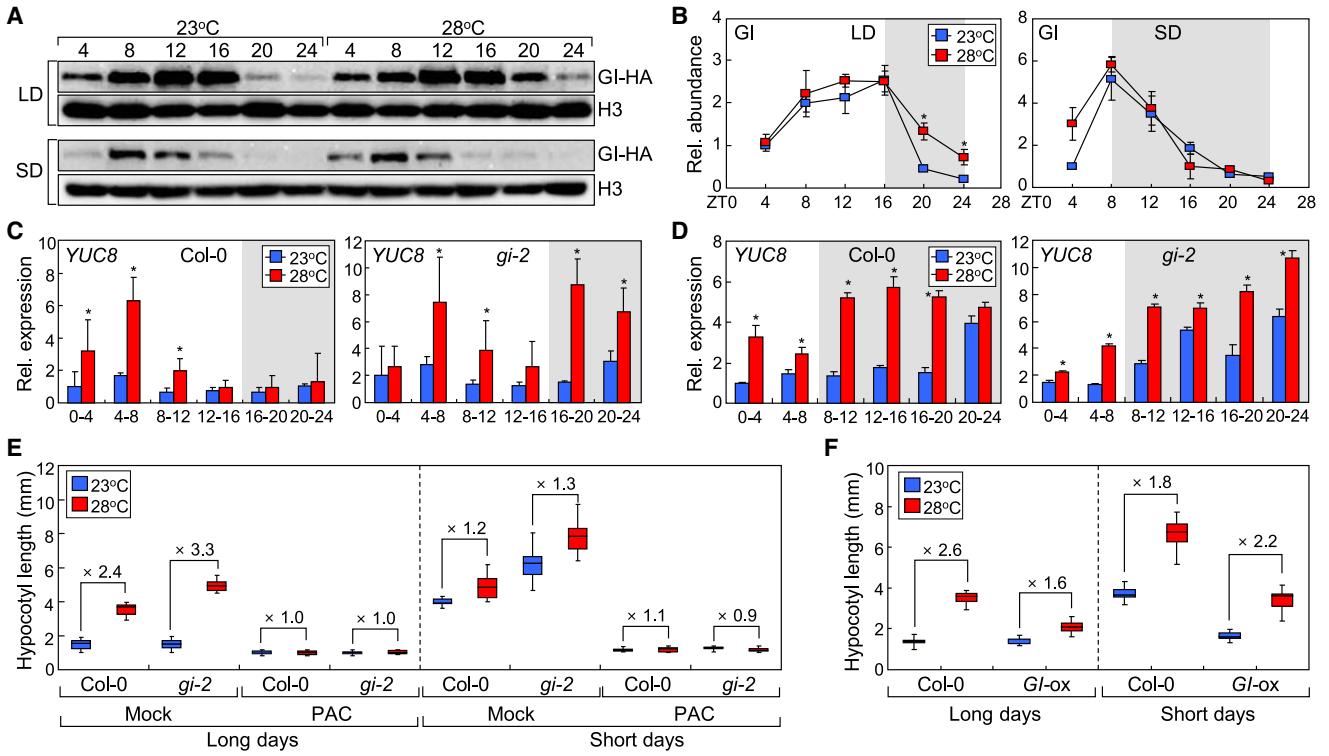

Figure 5. GI Converts Day-Length Information into Thermomorphogenesis.

(A and B) Diel patterns of GI accumulation. Five-day-old p*GI*:*GI-HA gi-2* seedlings grown at 23°C under either LDs or short days (SDs, 8-h light and 16-h dark) were subjected to temperature treatments. **(A)** GI-HA fusion proteins were immunodetected using an anti-HA antibody. H3 was included as loading control. **(B)** Protein bands were quantified and statistically analyzed (*t*-test, $*P < 0.01$, difference from 23°C). Error bars indicate SE. See also Supplemental Figure 5.

(C and D) Gating effects of warm temperatures on *YUC8* transcription. Six-day-old seedlings grown at 23°C under either LDs **(C)** or SDs **(D)** were subjected to 4-h temperature treatments during the time course. Transcript levels were analyzed by qRT–PCR (*t*-test, $*P < 0.01$, difference from 23°C). Error bars indicate SE.

(E) Thermomorphogenic hypocotyl growth of *gi-2* mutants under different day lengths. Three-day-old seedlings grown on MS-agar plates containing 0.2 mM PAC under either LDs or SDs were subjected to temperature treatments for 4 days under identical photoperiodic conditions. Numbers indicate fold changes.

(F) Thermomorphogenic hypocotyl growth of *GI*-ox seedlings. The *GI*-ox seedlings were grown and analyzed as described above.

notable that GI proteins are more abundant at 28°C than at 23°C during the nighttime under LDs (Figure 5A and 5B), which coincides with the timing of reduced RGA protein stability and increased thermomorphogenic responses in *gi-2* mutants (Figures 2E and 3C, respectively). These observations indicate that GI is thermally activated during hypocotyl thermomorphogenesis.

HEAT SHOCK PROTEIN 90 (HSP90) is a representative molecular chaperone that stabilizes a broad spectrum of cellular proteins in plants under high-temperature stress (Kim et al., 2011). It has recently been reported that GI functions alongside HSP90 during the maturation of ZTL proteins (Cha et al., 2017). As HSP90 accumulation is induced by warm temperatures (Wang et al., 2016), we examined whether HSP90 contributes to GI function during hypocotyl thermomorphogenesis.

We found that the thermally induced accumulation of HSP90 proteins was comparable in Col-0 and *gi-2* seedlings (Supplemental Figure 6A). While HSP90 is known to interact with GI, it did not interact with RGA in yeast cells (Supplemental Figure 6B). BiFC assays revealed that GI–HSP90 interactions occur in the nucleus at both 23°C and 28°C (Supplemental Figure 6C). Notably, the RGA protein abundance was slightly higher when seedlings were treated with an HSP90 inhibitor, geldanamycin (Supplemental Figure 6D), which is contrary to the reduction in RGA abundance found in *gi-2* mutants. These observations indicate that while HSP90 interacts with GI, it is not directly involved in the GI-mediated stabilization of RGA proteins during hypocotyl thermomorphogenesis. Instead, it is more likely that the intrinsic chaperone activity of GI is critical for the thermostabilization of the RGA protein.

GI Modulates the Day-Length-Dependent Gating of Temperature Responses

We observed that *gi-2* mutants exhibited hypocotyl overgrowth at warm temperatures, especially during ZT 16–24 under LDs (Figure 2B–2E), which is similar to the thermomorphogenic rhythms of wild-type seedlings grown under SDs (Box et al., 2015; Park et al., 2017). Therefore, the question remained as to whether and how GI-mediated day-length signals modulate the diel rhythms of thermomorphogenic growth.

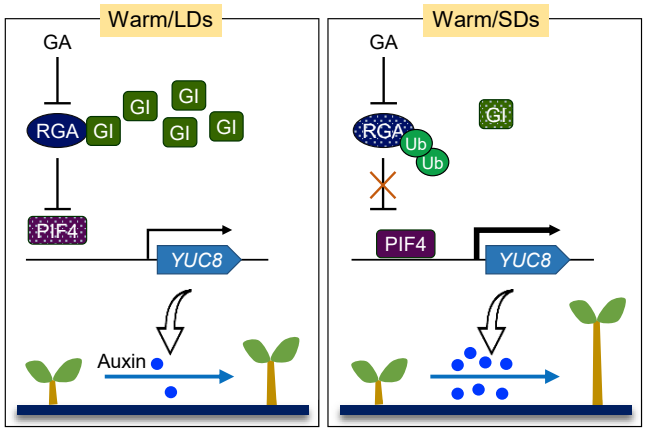

Figure 6. Working Model for GI-Mediated Photoperiodic Control of Thermomorphogenic Growth.

Under LDs, GI stabilizes RGA at warm temperatures. The thermostabilized RGA diminishes the DNA-binding affinity of PIF4, thus attenuating thermomorphogenic growth. Following the transition to SDs, GI is relatively unstable and its abundance is reduced. Consequently, RGA is readily degraded through the GA-mediated ubiquitination pathway, and the thermoactivated PIF4 induces *YUC8* transcription, promoting thermomorphogenic growth.

Circadian gating has previously been examined in order to explore the diel rhythms of hypocotyl thermomorphogenesis (Zhu et al., 2016; Park et al., 2017). Meanwhile, the circadian clock function of GI has been intensively functionally characterized (Cha et al., 2017). Therefore, we examined the potential roles of GI in modulating the gating of temperature responses by analyzing *YUC8* transcription under LDs and SDs.

Gating experiments revealed that exposure to warm temperatures during the day greatly enhanced *YUC8* transcription in Col-0 seedlings under LDs, but the promotive effects of warm temperatures were largely compromised during the night (Figure 5C). In contrast, the effects of thermal gating were evident during both the day and night in *gi-2* mutants under LDs (Figure 5C), which is consistent with the diel expression patterns of the *YUC8* and *SAUR22* genes and the diel rhythms of thermomorphogenic growth (Figure 2B–2E). Interestingly, under SDs, the effects of thermal gating were prominent during the night in Col-0 seedlings (Figure 5D), which is similar to what was observed in *gi-2* mutants under LDs (Figure 5C). Furthermore, while *gi-2* mutants still exhibited thermomorphogenic growth under SDs, the role of GI in hypocotyl thermomorphogenesis was more prominent under LDs than SDs (Figure 5E and 5F; Supplemental Figure 7A). In addition, we found that treatment with PAC abolished both photoperiodic- and warm-temperature-induced hypocotyl regulation in a DELLA-dependent manner (Figure 5E and Supplemental Figure 7B). Together, these observations indicate that GI mediates the photoperiodic control of thermal gating during hypocotyl thermomorphogenesis.

DISCUSSION

Thermomorphogenic adaptation responses help plants to efficiently manage body heat dissipation and leaf cooling, optimizing plant growth and fitness in warm climates (Crawford et al., 2012; Park et al., 2019). It has been documented that hypocotyl thermomorphogenesis primarily occurs during the middle of the day under LDs, when daily temperatures peak (Park et al., 2017). On the other hand, maximal hypocotyl growth is observed prior to dawn under SDs, ensuring that hypocotyl thermomorphogenesis occurs following a prolonged period of darkness (Nozue et al., 2007; Nusinow et al., 2011; Box et al., 2015; Park et al., 2017). Notably, the peak of thermomorphogenic hypocotyl growth strongly coincides with the maximal water availability under SDs (Nozue et al., 2007). Thus, it is apparent that shaping the diel rhythms of thermomorphogenic growth is critical for plant thermal adaptation.

In this study, we demonstrated that the GI-mediated photothermal regulation of DELLA stability serves as a signaling hub that integrates photoperiodic and temperature information into hypocotyl thermomorphogenesis. Our data illustrate how GI converts day-length information into RGA-mediated thermomorphogenic growth, shaping its photoperiodic rhythms (Figure 6). Under LDs, GI-mediated thermostabilization of RGA reduces the stability of PIF4, thereby attenuating thermomorphogenic growth. Consequently, hypocotyl elongation is finely adjusted to an optimal level, which is sufficient to support heat dissipation and leaf cooling and to prevent uncontrolled hypocotyl growth. On the other hand, under SDs, plants achieve maximal thermomorphogenic hypocotyl growth, which helps plants to absorb a sufficient amount of sunlight and ensure evaporative cooling. The GI-mediated shaping of photoperiodic rhythms during thermomorphogenic responses provides an adaptive advantage under changing environments, which are frequently encountered during seasonal transitions.

Our data also indicate that thermomorphogenic growth is not a simple thermoadaptation process but an intricate morphogenic system that is profoundly affected by day-length information. GI-mediated photoperiodic signals attenuate thermomorphogenic hypocotyl growth under LDs, which prevents unnecessary overgrowth and energy consumption, as has been noted previously (Lee et al., 2014). On the other hand, under SDs, GI abundance and stability are lessened, and thermomorphogenic hypocotyl growth occurs actively. As a result, plants are able to not only perceive sunlight efficiently but also readily dissipate heat.

Recently, an external coincidence model has been proposed in which hypocotyl thermomorphogenesis mostly occurs when temperature and photoperiodic cues coincide with one another (Park and Park, 2017), meaning that a potential photothermal modulator would be responsible for monitoring the coincidence of temperature and photoperiodic information (Martínez et al., 2018; Park and Park, 2019). Our data provide challenging evidence that GI is a critical component of the external coincidence model governing hypocotyl thermomorphogenesis in a day-length-dependent manner.

It is interesting that GI primarily modulates thermomorphogenic hypocotyl growth at night. Notably, it has been reported that the DELLA proteins mainly suppress hypocotyl growth at night, which coincides with the diel rhythmic reduction in DELLA

accumulation (Arana et al., 2011). This supports our observation that RGA proteins are rapidly degraded under warm LD conditions in *gi-2* mutants, which exhibit hypocotyl overgrowth at night. Therefore, the circadian oscillations of DELLA activity explain why *gi-2* mutants exhibit distinct diel rhythms of thermomorphogenic growth.

While the roles of GI in a variety of environmental adaptive mechanisms as well as in growth and developmental processes have been extensively studied for several decades, our understanding of the molecular and biochemical functions of GI is somewhat limited in most cases. One of the main reasons for this is poor identification of distinct functional domains in its protein structure (Mishra and Panigrahi, 2015). However, recent accumulating evidence suggests that the N-terminal region of GI is critical for its function. For example, it has been reported that GI is required for the FKF1-mediated degradation of CDF1 proteins, in which the N-terminal region of GI interacts directly with FKF1 (Sawa et al., 2007). In addition, the N-terminal region of GI has chaperone activity that is required for the maturation of ZTL proteins (Cha et al., 2017).

We demonstrated that the N-terminal region of GI interacts with RGA, which is important for the thermostabilization of RGA during hypocotyl thermomorphogenesis. It is possible that the chaperone activity of the N-terminal region protects substrate proteins, such as ZTL and RGA, from the ubiquitin-proteasome pathway or that it facilitates the functioning of FKF1 by forming active GI–FKF1 complexes (Sawa et al., 2007). Protein structural studies of the full-length GI protein or its N-terminal region will shed light on the functional mechanisms of GI. Recently, it has been shown that GI recruits the deubiquitylases UBIQUITIN-SPECIFIC PROTEASE 12 (UBP12) and UBP13 to stabilize the GI–ZTL protein complex (Lee et al., 2019). These deubiquitylases are also known to stabilize a jasmonate signaling component, a MYC2 transcription factor (Jeong et al., 2017), which directly interacts with RGA (Hong et al., 2012). Thus, the same deubiquitylases may be involved in the GI-mediated stabilization of its substrate proteins. GI is a plant-specific protein (Mishra and Panigrahi, 2015), and thus unraveling the molecular mechanisms underlying GI functions will also provide molecular clues as to the evolutionary relationships between plants and other eukaryotes.

GI interacts with multiple PIF proteins that mediate multiple facets of light-signaling events and accompanying photomorphogenic responses in plants (Nohales et al., 2019). GI regulates the functioning of its interacting partners by reducing their protein stability or by interfering with their DNA-binding ability. Our data indicate that GI attenuates PIF4 function by stabilizing DELLA proteins, which function as negative regulators of PIF proteins (Feng et al., 2008), during thermomorphogenesis. In addition, recent findings have shown that GI is also involved in GA signaling during photomorphogenesis through a similar mechanism (Nohales and Kay, 2019). It is thus likely that GI participates in a feedforward regulation loop consisting of the GI–PIF and GI–DELLA–PIF modules. It has been suggested that feedforward regulation is a highly robust mechanism that ensures the timely occurrence of molecular and biochemical events during leaf senescence (Kim et al., 2009). Similarly, we propose that the GI-mediated feedforward pathway directs thermomorphogenic growth to occur in a timely manner and at an optimal level during seasonal fluctuations.

Notably, a previous report has demonstrated that the functional roles of GI in GA signaling are at least partly linked with the *O*-fucosyltransferase SPY (Tseng et al., 2004). SPY induces the *O*-fucosylation of DELLA proteins, facilitating their efficient interaction with plant-growth-promoting transcription factors, such as BRASSINAZOLE-RESISTANT 1 (BZR1) and PIFs (Zentella et al., 2017). As GI directly interacts with SPY, it is conceivable that GI modulates the protein stability of SPY and the *O*-fucosylation of DELLA proteins. It is also possible that SPY induces the *O*-fucosylation of the GI protein, which would mediate the physical interactions between GI and DELLA proteins. Exploring these possibilities will lead to a more comprehensive understanding of the GI-mediated regulation of GA signaling.

GI is associated with low ambient temperature-responsive flowering (Jang et al., 2015). It also plays a role in warm-temperature-responsive flowering, independent of PIF4 (this work). In particular, different *gi* mutant alleles exhibit differential thermomorphogenic phenotypes, while they all exhibit delayed flowering. The question is whether GI-mediated flowering promotion is physiologically linked to GI-directed attenuation of thermomorphogenic growth. One plausible answer is that under warm-temperature conditions, plants utilize GI to accelerate flowering and simultaneously attenuate plant overgrowth through two distinct signaling pathways. It is also expected that the two GI-mediated developmental and adaptive processes are metabolically associated with one another: saving metabolic resources through the attenuation of thermomorphogenic growth would contribute to flowering acceleration. It is also worth investigating whether and how GI is functionally associated with the thermosensory flowering pathways that involve SHORT VEGETATIVE PHASE and FLOWERING LOCUS M (Lee et al., 2013; Posé et al., 2013).

METHODS

Plant Materials

All *Arabidopsis thaliana* lines used were in the Col-0 background except for the *sos2-2* mutant, which was generated in the Col-0 gl background, and the *dellaq* and *della* mutants, which were generated in the L*er* background (Cheng et al., 2004). The *gi-2* (CS3397), *ft-10* (CS9869), *ztl-105* (SALK-069091), *gi-1* (CS3123), *gi-201* (SALK-092757), and *della* (CS16298) mutants were obtained from a pool of mutant lines deposited in the Arabidopsis Biological Resource Center (Ohio State University, Columbus, OH). The *co-101* and *pif4-101* (Garlic-114-G06) mutants have been described previously (Takada and Goto, 2003; Lorrain et al., 2008). The *sos2-2* mutant and Col-0 gl seeds were obtained from Dae-Jin Yun. The *rga-28* and *rga-28 gai-t6* mutants were obtained from Giltsu Choi. The *gi-2 pif4-101* double mutant was generated by a genetic cross between the *gi-2* and *pif4-101* mutants. To generate GI-overexpressing (*GI*-ox) plants, we subcloned a GI-coding sequence under the control of the cauliflower mosaic virus (CaMV) 35S promoter in the pB2GW7 vector. The expression construct was transformed into Col-0 plants. The p*GI*:*GI-HA gi-2* transgenic plants were described previously (Kang et al., 2015). The p*RGA*:*GFP-RGA* transgenic plants were obtained from a seed stock deposited in the Nottingham Arabidopsis Stock Center (University of Nottingham, Sutton Bonington Campus, UK).

Plant Growth Conditions

Sterilized *Arabidopsis* seeds were cold-stratified for 3 days and were allowed to germinate on half-strength Murashige and Skoog agar (hereafter referred to as MS-agar) plates under either LDs (16-h light and 8-h dark) or SDs (8-h light and 16-h dark) with white light (120 μmol m^{-2} s^{-1}) provided by fluorescent FLR40D/A tubes (Osram, Seoul, Korea) in a controlled growth chamber set at 23°C. For phenotypic assays, 3-day-old seedlings were further grown at either 23°C or 28°C under either LDs or SDs for 4 additional days. To prepare total RNA and protein samples, we transferred 5-day-old seedlings to either 23°C or 28°C for the indicated time periods before harvesting whole seedlings.

Phenotyping

Hypocotyl length, leaf span, and leaf angle were analyzed using digital images of 7-day-old seedlings. To examine the effects of chemicals on plant growth and morphology, we grew seedlings on MS-agar plates containing either 10 μM 1–naphthylphthalamic acid (NPA (Chem Service, N-12507) or 0.2 μM paclobutrazol (PAC) (Sigma-Aldrich, 46046). Quantification of thermomorphogenic hypocotyl phenotypes was performed using ImageJ software (http://imagej.nih.gov/ij/).

For flowering time measurements, plants were germinated and grown in soil until flowering under LDs at either 23°C or 28°C. Total leaf numbers of 16 individual plants were counted and statistically analyzed.

Gene Expression Analyses

Plant materials were ground in liquid nitrogen, and the ground plant material was thoroughly suspended in 1 ml of TRIzol reagent (Invitrogen, 15596018). The suspension was centrifuged at 16 000 *g* for 10 min at 4°C. The supernatant was mixed with 200 μl of chloroform and centrifuged again under identical conditions. After centrifugation, 400 μl of the aqueous phase was transferred to an unused microcentrifuge tube containing 200 μl of high-salt solution (0.8 M trisodium citrate, 1.2 M sodium chloride) and 200 μl of isopropanol. After incubation for 15 min at room temperature, tubes were centrifuged at 16 000 *g* for 10 min at 4°C. The RNA pellet was washed with 75% ethanol and dissolved in deionized water.

Transcript levels were analyzed by reverse transcription-mediated quantitative PCR (qRT–PCR) according to the guidelines proposed to assure reproducible measurements of relative RNA levels (Udvardi et al., 2008). qRT–PCR reactions were conducted in 384-well blocks with the QuantStudio 6 Flex system (Applied Biosystems, Foster City, CA) using the SYBR Green I master mix (KAPA Biosystems, KM4101) in a volume of 10 μl. The two-step thermal cycling profile employed was 15 s at 95°C for denaturation and 1 min at 60°C–65°C for primer annealing and polymerization, depending on the calculated melting temperatures of the PCR primers. The PCR primers used are listed in Supplemental Table 1. The *Arabidopsis eIF4A* gene (At3g13920) was included as an internal control in individual PCR reactions to normalize for variation in the amount of primary cDNA sample used.

All qRT–PCR reactions were run in biological triplicates using total RNA samples prepared separately from independent plant materials that were grown under identical experimental conditions. The comparative $\Delta\Delta C_T$ method was employed to evaluate the relative quantities of each amplified product in the samples. The threshold cycle (C_T) was automatically determined for each reaction by the system set with default parameters.

Measurement of Hypocotyl Growth Kinetics

Two-day-old seedlings grown on vertical MS-agar plates at 23°C were further grown at either 23°C or 28°C before infrared photographs were taken. Following plant exposure to different temperature regimes, photographs were taken every 30 min for up to 3 days using a Nature view HD Live View camera (Bushnell, Overland Park, KS) under infrared light, as described previously (Park et al., 2017). The images were analyzed using ImageJ software.

Immunological Assays

Five-day-old seedlings grown at 23°C were further grown at either 23°C or 28°C for the indicated time periods before whole seedlings were harvested for total protein extraction. For PAC treatments, seedlings were grown on MS-agar plates containing 0.2 μM PAC. Total protein extraction was performed as described previously (Park et al., 2017). Anti-RGA (Agrisera, AS11 1630), anti-PIF4 (Abiocode, R2534-4), anti-HSP90 (Agrisera, AS08 346), anti-HA (Millipore, 05-904), and anti-H3 (Abcam, Ab1791) antibodies were used for the immunological detection of the RGA, PIF4, HSP90.1, HA, and H3 proteins, respectively. An anti-rabbit IgG-peroxidase antibody (Millipore, AP132P) was used as the secondary antibody for the immunoblot assays with anti-RGA, anti-PIF4, anti-HSP90, and anti-H3 primary antibodies. An anti-mouse IgG-peroxidase antibody (Millipore, AP124P) was used as the secondary antibody in immunoblot assays with anti-HA and anti-GFP primary antibodies (Santa Cruz Biotechnology, sc-9996).

Co-immunoprecipitation (coIP) assays were performed similarly as previously described (Lee et al., 2014). Seven-day-old, warm-temperature-treated seedlings grown on MS-agar plates were harvested and ground in liquid nitrogen. The ground plant material was resuspended in 30 ml of nuclear extraction buffer (1.7 M sucrose, 10 mM Tris–Cl [pH 7.5], 2 mM $MgCl_2$, 0.15% Triton X-100, 5 mM β-mercaptoethanol, and 0.1 mM PMSF) containing protease inhibitors. The suspensions were filtered through Miracloth filters. The filtered mixture was then centrifuged at 4300 *g* for 20 min at 4°C, and nuclear fractions were isolated using the sucrose cushion method. The nuclear fractions were lysed and sonicated in coIP buffer (1 mM EDTA, 10% glycerol, 75 mM NaCl, 0.1 M Tris–Cl [pH 7.5], and 0.1% Triton X-100) containing protease inhibitors. A portion of the sonicated solution was used as the input sample. Five micrograms of an anti-HA antibody (Millipore) was added to the protein solution and the solution was incubated for 8 h at 4°C. Protein-G magnetic beads (Bio-Rad, 161-4023) were then added to the solution and incubated for 3 h. The beads were precipitated using a magnetic rack and were washed with coIP wash buffer six times. Subsequently, 2× SDS–PAGE loading buffer was added to the washed beads. The resulting protein solution was used as the IP sample. To determine the amounts of co-immunoprecipitated proteins, we performed western blot assays.

Yeast Two-Hybrid Assays

Yeast two-hybrid assays were performed using the Clontech Matchmaker system (Mountain View, CA). The pGADT7 and pGBKT7 vectors were used for the GAL4 activation domain and GAL4 binding domain, respectively. Yeast strain AH109 (Leu-, Trp-, Ade-, His-), which harbors chromosomally integrated reporter genes *lacZ* and *HIS* under the control of the GAL1 promoter, was used for transformation. Transformation of AH109 cells was performed according to the manufacturer's procedure. Colonies obtained were restreaked on a medium lacking Leu, Trp, Ade, and His. To eliminate nonspecific growth, we included 3-amino-1,2,4-triazole (3-AT) (Sigma-Aldrich, A8056) in the growth medium at appropriate concentrations.

Bimolecular Fluorescence Complementation Assays

The full-length *GI* coding sequence was fused in frame to the 3′ end of a gene sequence encoding the N-terminal half of enhanced YFP in the pSATN-nEYFP-C1 vector (Lee et al., 2014). The coding sequence of full-length *RGA* or *HSP90.1* was fused in frame to the 3′ end of a gene sequence encoding the C-terminal half of enhanced YFP in the pSATN-cEYFP-C1 vector. The p2RGW7 vector harboring the *RFP-SPCH* gene fusion under the control of the CaMV 35S promoter was included as a nuclear marker in the assays (Park et al., 2017). The expression constructs were co-transformed into *Arabidopsis* mesophyll protoplasts using the polyethylene glycol–calcium transfection method as described previously

(Park et al., 2017). Transformed protoplasts were incubated at either 23°C or 28°C for 1 day. Optical images and RFP and YFP fluorescence images were obtained using a Carl Zeiss LSM710 microscope (Jena, Germany) with the following laser and filter setup parameters: 543 nm for excitation, 561–703 nm for emission to detect RFP, 488 nm for excitation, and 493–543 nm for emission to detect YFP.

Statistical Analyses

The statistical significance of differences between means was determined using two-sided Student's *t*-tests with *P* values of <0.01. To determine statistical significance of differences for more than two populations, we used one-way analysis of variance (ANOVA) with post hoc Tukey tests ($P < 0.05$). Statistical analyses were performed using Rstudio software (https://www.rstudio.com/).

ACCESSION NUMBERS

The accession numbers of genes in this article are: *GI*, AT1G22770; *RGA*, AT2G01570; *GAI*, AT1G14920; *RGL1*, AT1G66350; *RGL2*, AT3G03450; *RGL3*, AT5G17490; *HSP90*, AT1G04130; *PIF4*, AT2G43010; *PIF5*, AT3G59060; *YUC8*, AT4G28720; *SAUR22*, AT5G18050.

SUPPLEMENTAL INFORMATION

Supplemental Information is available at *Molecular Plant Online*.

FUNDING

This work was supported by the Leaping Research (NRF-2018R1A2A1A19020840) Program provided by the National Research Foundation of Korea (NRF) and the Next-Generation BioGreen 21 Program (PJ013134) provided by the Rural Development Administration of Korea. Y.-J.P. was partially supported by Global PhD Fellowship Program through NRF (NRF-2016H1A2A1906534).

AUTHOR CONTRIBUTIONS

C.-M.P., and Y.-J.P. conceived and designed the experiments. C.-M.P. prepared the manuscript with contributions from Y.-J.P. and J.Y.K. Y.-J.P. carried out thermomorphogenic and biochemical assays with contributions from J.Y.K. and J.-H.L. Y.-J.P. and J.Y.K. analyzed data. B.-D.L. and N.-C.P. managed plant materials and participated in scientific discussions.

ACKNOWLEDGMENTS

We thank Dae-Jin Yun for providing *sos2-2* mutants and their parental Col-0 gl seeds. We also thank Giltsu Choi for providing *rga-28* and *rga-28 gai-t6* mutant seeds. No conflict of interest declared.

Received: September 16, 2019
Revised: December 25, 2019
Accepted: January 10, 2020
Published: January 16, 2020

REFERENCES

Arana, M.V., Marín-de la Rosa, N., Maloof, J.N., Blázquez, M.A., and Alabadí, D. (2011). Circadian oscillation of gibberellin signaling in *Arabidopsis*. Proc. Natl. Acad. Sci. U S A **108**:9292–9297.

Box, M.S., Huang, B.E., Domijan, M., Jaeger, K.E., Khattak, A.K., Yoo, S.J., Sedivy, E.L., Jones, D.M., Hearn, T.J., Webb, A.A.R., et al. (2015). ELF3 controls thermoresponsive growth in *Arabidopsis*. Curr. Biol. **25**:194–199.

Cha, J.Y., Kim, J., Kim, T.S., Zeng, Q., Wang, L., Lee, S.Y., Kim, W.Y., and Somers, D.E. (2017). GIGANTEA is a co-chaperone which facilitates maturation of ZEITLUPE in the *Arabidopsis* circadian clock. Nat. Commun. **8**:3.

Cheng, H., Qin, L., Lee, S., Fu, X., Richards, D.E., Cao, D., Luo, D., Harberd, N.P., and Peng, J. (2004). Gibberellin regulates *Arabidopsis* floral development via suppression of DELLA protein function. Development **131**:1055–1064.

Crawford, A.J., McLachlan, D.H., Hetherington, A.M., and Franklin, K.A. (2012). High temperature exposure increases plant cooling capacity. Curr. Biol. **22**:R396–R397.

Davière, J.M., and Achard, P. (2013). Gibberellin signaling in plants. Development **140**:1147–1151.

Delker, C., Sonntag, L., James, G.V., Janitza, P., Ibañez, C., Ziermann, H., Peterson, T., Denk, K., Mull, S., Ziegler, J., et al. (2014). The DET1-COP1-HY5 pathway constitutes a multipurpose signaling module regulating plant photomorphogenesis and thermomorphogenesis. Cell Rep. **9**:1983–1989.

de Lucas, M., Davière, J.M., Rodríguez-Falcón, M., Pontin, M., Iglesias-Pedraz, J.M., Lorrain, S., Fankhauser, C., Blázquez, M.A., Titarenko, E., and Prat, S. (2008). A molecular framework for light and gibberellin control of cell elongation. Nature **451**:480–484.

Dill, A., Thomas, S.G., Hu, J., Steber, C.M., and Sun, T.P. (2004). The *Arabidopsis* F-box protein SLEEPY1 targets gibberellin signaling repressors for gibberellin-induced degradation. Plant Cell **16**:1392–1405.

Feng, S., Martinez, C., Gusmaroli, G., Wang, Y., Zhou, J., Wang, F., Chen, L., Yu, L., Iglesias-Pedraz, J.M., Kircher, S., et al. (2008). Coordinated regulation of *Arabidopsis thaliana* development by light and gibberellins. Nature **451**:475–479.

Franklin, K.A., Lee, S.H., Patel, D., Kumar, S.V., Spartz, A.K., Gu, C., Ye, S., Yu, P., Breen, G., Cohen, J.D., et al. (2011). Phytochrome-interacting factor 4 (PIF4) regulates auxin biosynthesis at high temperature. Proc. Natl. Acad. Sci. U S A **108**:20231–20235.

Griffiths, J., Murase, K., Rieu, I., Zentella, R., Zhang, Z.L., Powers, S.J., Gong, F., Phillips, A.L., Hedden, P., Sun, T.P., et al. (2006). Genetic characterization and functional analysis of the GID1 gibberellin receptors in *Arabidopsis*. Plant Cell **18**:3399–3414.

Hong, G.J., Xue, X.Y., Mao, Y.B., Wang, L.J., and Chen, X.Y. (2012). *Arabidopsis* MYC2 interacts with DELLA proteins in regulating sesquiterpene synthase gene expression. Plant Cell **24**:2635–2648.

Huang, J., Yu, H., Dai, A., Wei, Y., and Kang, L. (2017). Drylands face potential threat under 2 °C global warming target. Nat. Clim. Change **7**:417–422.

Jang, K., Lee, H.G., Jung, S.J., Paek, N.C., and Seo, P.J. (2015). The E3 ubiquitin ligase COP1 regulates thermosensory flowering by triggering GI degradation in *Arabidopsis*. Sci. Rep. **5**:12071.

Jeong, J.S., Jung, C., Seo, J.S., Kim, J.K., and Chua, N.H. (2017). The deubiquitinating enzymes UBP12 and UBP13 positively regulate MYC2 levels in jasmonate responses. Plant Cell **29**:1406–1424.

Jung, J.H., Domijan, M., Klose, C., Biswas, S., Ezer, D., Gao, M., Khattak, A.K., Box, M.S., Charoensawan, V., Cortijo, S., et al. (2016). Phytochromes function as thermosensors in *Arabidopsis*. Science **354**:886–889.

Kang, M.Y., Yoo, S.C., Kwon, H.Y., Lee, B.D., Cho, J.N., Noh, Y.S., and Paek, N.C. (2015). Negative regulatory roles of DE-ETIOLATED1 in flowering time in *Arabidopsis*. Sci. Rep. **5**:9728.

Kim, W.Y., Fujiwara, S., Suh, S.S., Kim, J., Kim, Y., Han, L., David, K., Putterill, J., Nam, H.G., and Somers, D.E. (2007). ZEITLUPE is a circadian photoreceptor stabilized by GIGANTEA in blue light. Nature **449**:356–360.

Kim, J.H., Woo, H.R., Kim, J., Lim, P.O., Lee, I.C., Choi, S.H., Hwang, D., and Nam, H.G. (2009). Trifurcate feed-forward regulation of age-dependent cell death involving miR164 in *Arabidopsis*. Science **323**:1053–1057.

Kim, T.S., Kim, W.Y., Fujiwara, S., Kim, J., Cha, J.Y., Park, J.H., Lee, S.Y., and Somers, D.E. (2011). HSP90 functions in the circadian

clock through stabilization of the client F-box protein ZEITLUPE. Proc. Natl. Acad. Sci. U S A **108**:16843–16848.

Kim, W.Y., Ali, Z., Park, H.J., Park, S.J., Cha, J.Y., Perez-Hormaeche, J., Quintero, F.J., Shin, G., Kim, M.R., Qiang, Z., et al. (2013). Release of SOS2 kinase from sequestration with GIGANTEA determines salt tolerance in *Arabidopsis*. Nat. Commun. **4**:1352.

Koini, M.A., Alvey, L., Allen, T., Tilley, C.A., Harberd, N.P., Whitelam, G.C., and Franklin, K.A. (2009). High temperature-mediated adaptations in plant architecture require the bHLH transcription factor PIF4. Curr. Biol. **19**:408–413.

Kumar, S.V., Lucyshyn, D., Jaeger, K.E., Alós, E., Alvey, E., Harberd, N.P., and Wigge, P.A. (2012). Transcription factor PIF4 controls the thermosensory activation of flowering. Nature **484**:242–245.

Lee, J.H., Ryu, H.S., Chung, K.S., Posé, D., Kim, S., Schmid, M., and Ahn, J.H. (2013). Regulation of temperature-responsive flowering by MADS-box transcription factor repressors. Science **342**:628–632.

Lee, H.J., Jung, J.H., Cortés Llorca, L., Kim, S.G., Lee, S., Baldwin, I.T., and Park, C.M. (2014). FCA mediates thermal adaptation of stem growth by attenuating auxin action in *Arabidopsis*. Nat. Commun. **5**:5473.

Lee, C.M., Li, M.W., Feke, A., Liu, W., Saffer, A.M., and Gendron, J.M. (2019). GIGANTEA recruits the UBP12 and UBP13 deubiquitylases to regulate accumulation of the ZTL photoreceptor complex. Nat. Commun. **10**:3750.

Li, K., Yu, R., Fan, L.M., Wei, N., Chen, H., and Deng, X.W. (2016). DELLA-mediated PIF degradation contributes to coordination of light and gibberellin signalling in *Arabidopsis*. Nat. Commun. **7**:11868.

Lorrain, S., Allen, T., Duek, P.D., Whitelam, G.C., and Fankhauser, C. (2008). Phytochrome-mediated inhibition of shade avoidance involves degradation of growth-promoting bHLH transcription factors. Plant J. **53**:312–323.

Martínez, C., Nieto, C., and Prat, S. (2018). Convergent regulation of PIFs and the E3 ligase COP1/SPA1 mediates thermosensory hypocotyl elongation by plant phytochromes. Curr. Opin. Plant Biol. **45**:188–203.

Martin-Tryon, E.L., Kreps, J.A., and Harmer, S.L. (2007). GIGANTEA acts in blue light signaling and has biochemically separable roles in circadian clock and flowering time regulation. Plant Physiol. **143**:473–486.

Mishra, P., and Panigrahi, K.C. (2015). GIGANTEA—an emerging story. Front. Plant Sci. **6**:8.

Nohales, M.A., and Kay, S.A. (2019). GIGANTEA gates gibberellin signaling through stabilization of the DELLA proteins in *Arabidopsis*. Proc. Natl. Acad. Sci. U S A **116**:21893–21899.

Nohales, M.A., Liu, W., Duffy, T., Nozue, K., Sawa, M., Pruneda-Paz, J.L., Maloof, J.N., Jacobsen, S.E., and Kay, S.A. (2019). Multi-level modulation of light signaling by GIGANTEA regulates both the output and pace of the circadian clock. Dev. Cell **49**:840–851.

Nozue, K., Covington, M.F., Duek, P.D., Lorrain, S., Fankhauser, C., Harmer, S.L., and Maloof, J.N. (2007). Rhythmic growth explained by coincidence between internal and external cues. Nature **448**:358–361.

Nusinow, D.A., Helfer, A., Hamilton, E.E., King, J.J., Imaizumi, T., Schultz, T.F., Farré, E.M., and Kay, S.A. (2011). The ELF4-ELF3-LUX complex links the circadian clock to diurnal control of hypocotyl growth. Nature **475**:398–402.

Park, Y.J., and Park, C.M. (2017). External coincidence model for hypocotyl thermomorphogenesis. Plant Signal. Behav. **13**:e1327498.

Park, Y.J., and Park, C.M. (2019). Physicochemical modeling of the phytochrome-mediated photothermal sensing. Sci. Rep. **9**:10485.

Park, Y.J., Lee, H.J., Ha, J.H., Kim, J.Y., and Park, C.M. (2017). COP1 conveys warm temperature information to hypocotyl thermomorphogenesis. New Phytol. **215**:269–280.

Park, Y.J., Lee, H.J., Gil, K.E., Kim, J.Y., Lee, J.H., Lee, H., Cho, H.T., Vu, L.D., De Smet, I., and Park, C.M. (2019). Developmental programming of thermonastic leaf movement. Plant Physiol. **180**:1185–1197.

Peng, S., Huang, J., Sheehy, J.E., Laza, R.C., Visperas, R.M., Zhong, X., Centeno, G.S., Khush, G.S., and Cassman, K.G. (2004). Rice yields decline with higher night temperature from global warming. Proc. Natl. Acad. Sci. U S A **101**:9971–9975.

Posé, D., Verhage, L., Ott, F., Yant, L., Mathieu, J., Angenent, G.C., Immink, R.G., and Schmid, M. (2013). Temperature-dependent regulation of flowering by antagonistic FLM variants. Nature **503**:414–417.

Sawa, M., and Kay, S.A. (2011). GIGANTEA directly activates Flowering Locus T in *Arabidopsis thaliana*. Proc. Natl. Acad. Sci. U S A **108**:11698–11703.

Sawa, M., Nusinow, D.A., Kay, S.A., and Imaizumi, T. (2007). FKF1 and GIGANTEA complex formation is required for day-length measurement in *Arabidopsis*. Science **318**:261–265.

Song, Y.H., Smith, R.W., To, B.J., Millar, A.J., and Imaizumi, T. (2012). FKF1 conveys timing information for CONSTANS stabilization in photoperiodic flowering. Science **336**:1045–1049.

Stavang, J.A., Gallego-Bartolomé, J., Gómez, M.D., Yoshida, S., Asami, T., Olsen, J.E., García-Martínez, J.L., Alabadí, D., and Blázquez, M.A. (2009). Hormonal regulation of temperature-induced growth in *Arabidopsis*. Plant J. **60**:589–601.

Sun, J., Qi, L., Li, Y., Chu, J., and Li, C. (2012). PIF4-mediated activation of YUCCA8 expression integrates temperature into the auxin pathway in regulating *Arabidopsis* hypocotyl growth. PLoS Genet. **8**:e1002594.

Takada, S., and Goto, K. (2003). Terminal flower2, an *Arabidopsis* homolog of heterochromatin protein1, counteracts the activation of flowering locus T by constans in the vascular tissues of leaves to regulate flowering time. Plant Cell **15**:2856–2865.

Tseng, T.S., Salomé, P.A., McClung, C.R., and Olszewski, N.E. (2004). SPINDLY and GIGANTEA interact and act in *Arabidopsis thaliana* pathways involved in light responses, flowering, and rhythms in cotyledon movements. Plant Cell **16**:1550–1563.

Tyler, L., Thomas, S.G., Hu, J., Dill, A., Alonso, J.M., Ecker, J.R., and Sun, T.P. (2004). Della proteins and gibberellin-regulated seed germination and floral development in *Arabidopsis*. Plant Physiol. **135**:1008–1019.

Udvardi, M.K., Czechowski, T., and Scheible, W.R. (2008). Eleven golden rules of quantitative RT-PCR. Plant Cell **20**:1736–1737.

Wang, R., Zhang, Y., Kieffer, M., Yu, H., Kepinski, S., and Estelle, M. (2016). HSP90 regulates temperature-dependent seedling growth in *Arabidopsis* by stabilizing the auxin co-receptor F-box protein TIR1. Nat. Commun. **7**:10269.

Yu, J.W., Rubio, V., Lee, N.Y., Bai, S., Lee, S.Y., Kim, S.S., Liu, L., Zhang, Y., Irigoyen, M.L., Sullivan, J.A., et al. (2008). COP1 and ELF3 control circadian function and photoperiodic flowering by regulating GI stability. Mol. Cell **32**:617–630.

Zentella, R., Sui, N., Barnhill, B., Hsieh, W.P., Hu, J., Shabanowitz, J., Boyce, M., Olszewski, N.E., Zhou, P., Hunt, D.F., et al. (2017). The *Arabidopsis* O-fucosyltransferase SPINDLY activates nuclear growth repressor DELLA. Nat. Chem. Biol. **13**:479–485.

Zhu, J.Y., Oh, E., Wang, T., and Wang, Z.Y. (2016). TOC1-PIF4 interaction mediates the circadian gating of thermoresponsive growth in *Arabidopsis*. Nat. Commun. **7**:13692.